Helicity conservation in topology-changing reconnections: the flow of linking and coiling across scales

Martin W. Scheeler,[1,*] Dustin Kleckner*,[1,†] Davide Proment,[2] Gordon L. Kindlmann,[3] and William T.M. Irvine[1,‡]

[1] *James Franck Institute, Department of Physics,*
The University of Chicago, Chicago, Illinois 60637, USA.
[2] *School of Mathematics, The University of East Anglia, NR4 7TJ Norwich, Norfolk, UK.*
[3] *Computation Institute, Department of Computer Science,*
The University of Chicago, Chicago, Illinois 60637, USA.

The conjecture that knottedness is a fundamental conserved physical quantity has a long history in fluid mechanics. In ideal flows, the conservation of helicity arises because the topology of vortex lines is invariant. In real flows (including superfluids), the large scale topology of vortex tubes changes through 'reconnection' events, so helicity can only be conserved by transferring to different spatial scales. By measuring the behavior of vortex knots and links in viscous fluid experiments and quantum fluid simulations, we identify a mechanism for helicity scale transfer through reconnections, allowing helicity to be conserved even when the topology is not. We also describe a new method for quantifying helicity across scales, and discuss the transfer of helicity to sub-core local twisting where it may ultimately be dissipated. Remarkably, we find that topology-changing reconnections proceed in a manner than tends to conserve helicity, suggesting that it plays a fundamental role in real fluids, from turbulent viscous flows to plasmas.

In addition to energy, momentum and angular momentum, ideal (inviscid) fluids have an additional conserved quantity – helicity (eqn. 1) – which measures the linking and knotting of the vortex lines composing a flow [1]. For an ideal fluid, the conservation of helicity is a direct consequence of the Helmholtz laws of vortex motion, which both forbid vortex lines from ever crossing and preserve the flux of vorticity, making it impossible for linked or knotted vortices to ever untie [1, 2]. Since conservation laws are of fundamental importance in understanding flows, the question of whether this topological conservation law extends to real, dissipative systems is of clear and considerable interest. The general importance of this question is further underscored by the recent and growing impact knots and links are having across a range of fields, including plasmas [3, 4], liquid crystals [5, 6], optical [7], electromagnetic [8] and biological structures [9–11], cosmic strings [12, 13] and beyond [14]. Determining if and how helicity is conserved in the presence of dissipation is therefore paramount in understanding the fundamental dynamics of real fluids and the connections between tangled fields across systems.

The robustness of helicity conservation in real fluids is unclear because dissipation allows the topology of field lines to change. For example, in viscous flows vorticity will diffuse, allowing nearby vortex tubes to 'reconnect' (Fig. 1), creating or destroying the topological linking of vortices. This behavior is not unique to classical fluids: analogous reconnection events have also been experimentally observed in superfluids [15] and coronal loops of plasma on the surface of the sun [16]. In general, these observed reconnection events exhibit divergent, non-linear dynamics which makes it difficult to resolve these questions theoretically [4, 17, 18]. On the other hand, experimental tests of helicity conservation have been hindered by the lack of techniques to create vortices with topological structure. Thanks to a recent advance [19], this is finally possible.

While on the one hand the diffusion of vorticity enables reconnections that remove topology, it also guarantees that vortex tubes have finite thickness. Finite thickness allows for internal structure – like the filaments that make up a strand of yarn – which may also store helicity [20–22]. When topology changes through a reconnection event, helicity conservation is therefore dependent on whether and how global linking is transferred to this interior structure.

By performing experiments on linked and knotted vortices in water, as well as numerical simulations of Bose-Einstein condensates (a compressible superfluid [23]) and Biot-Savart vortex evolution, we investigate the conservation of helicity, in so far as it can be inferred from the shape of the reconnecting flux tubes. We report a system-independent geometric mechanism for helicity conservation through a reconnection. We also describe a new method for quantifying the storage of helicity on different spatial scales of a thin-core vortex: a 'helistogram'. Using this analysis technique, we find that self-induced vortex stretching generates a rich structure in the flow of helicity, driving both vortex reconnections and geometric deformations that transport helicity between scales.

The hydrodynamic helicity is defined in terms of the fluid flow field, $\boldsymbol{u}(\boldsymbol{r})$:

$$\mathcal{H} = \int \boldsymbol{u} \cdot \boldsymbol{\omega} \; dV, \tag{1}$$

where the vorticity is $\boldsymbol{\omega}(\boldsymbol{r}) = \boldsymbol{\nabla} \times \boldsymbol{u}(\boldsymbol{r})$. The connection between this volumetric representation and the linking between vortex tubes was first noted by Moffatt [1], who showed that for flows consisting of thin, closed vortex

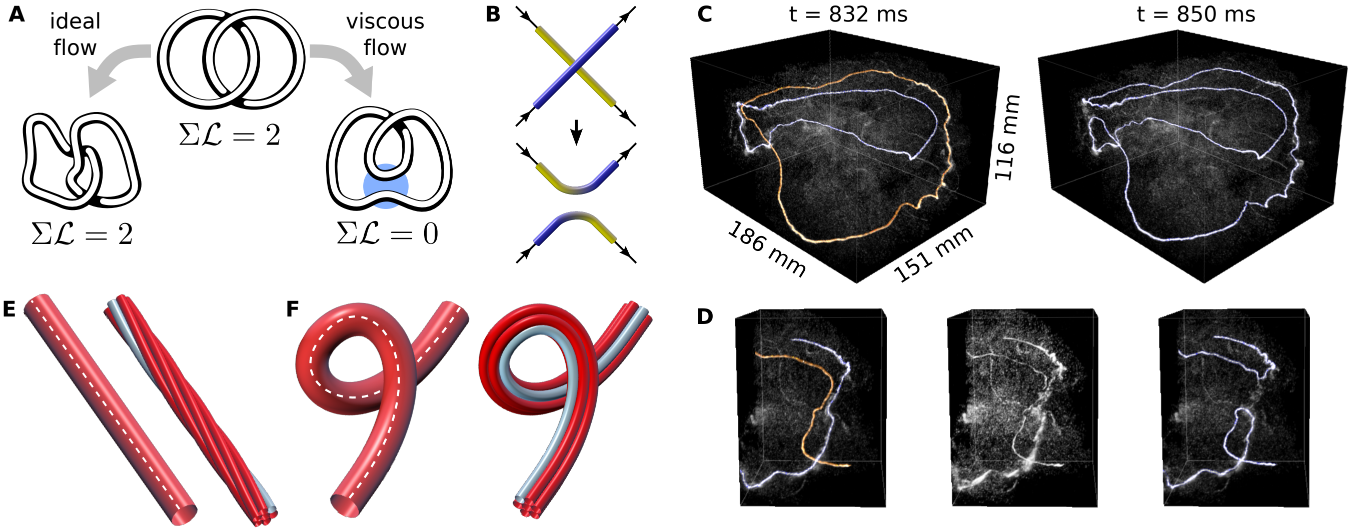

FIG. 1: (**A**) A sketch of the evolution of vortex tube topology in ideal (Euler) and viscous (Navier-Stokes) flow. Dissipative flows allow for reconnections of vortex tubes (highlighted in blue), and so topology is not conserved. (**B**) A diagram of a single reconnection event. (**C**) Two frames of a 3D reconstruction of a vortex reconnection in experiment, which turns an initially linked pair of rings into a single twisted ring. (**D**) A close-up view of the reconnection in **C**. (**E**) Vortex 'tubes' may contain internal structure even when their centerline is straight, leading to the storage of helicity as twist. (**F**) If the vortex tube 'writhes', it may store helicity even when the topology of the centerline is trivial.

tubes $\mathcal{C}_n$, with compact internal structure, the helicity is equivalently given by:

$$\mathcal{H} = \sum_{i,j} \Gamma_i \Gamma_j \frac{1}{4\pi} \oint_{\mathcal{C}_i} \oint_{\mathcal{C}_j} \frac{\boldsymbol{x}_i - \boldsymbol{x}_j}{|\boldsymbol{x}_i - \boldsymbol{x}_j|^2} \cdot (d\boldsymbol{x}_i \times d\boldsymbol{x}_j) \qquad (2)$$

$$= \sum_{i \neq j} \Gamma_i \Gamma_j \; \mathcal{L}_{ij} + \sum_i \Gamma_i^2 \; \mathcal{W}r_i. \qquad (3)$$

where Γ_i and $\boldsymbol{x}_i$ correspond to the circulation (vorticity flux) and center-line path for vortex tube $\mathcal{C}_i$, and we have assumed that each vortex-tube is locally untwisted and non-intersecting. The linking number, $\mathcal{L}_{ij}$, is a topological invariant which measures the signed integer number of times a pair of closed tubes is wrapped around one another. The writhe, $\mathcal{W}r_i$, is an analogous quantity for a single path, which includes contributions from both knotting and helix-like coiling, and in general is not integer.

If a vortex tube has finite thickness, the vortex 'bundle' (with total circulation Γ) can be mathematically decomposed into 'filaments' (each with $\Gamma_{filament} = \Gamma/N$) that describe its internal structure. As the number of filaments increases, $N \to \infty$, the writhe contribution to the helicity is seen to vanish, replaced by the linking between individual filaments inside the bundle [21]. Thus a vortex tube whose internal filaments are linked stores topology even though its centerline is topologically trivial. For example, in a vortex loop whose centerline has no torsion, such as a circle, internal topology can be achieved by uniformly twisting the vortex sub-tubes around each other (Fig. 1**E**). Conversely, the same topology can be achieved without internal twisting if instead the vortex bundle writhes in space (Fig. 1**F**). In this sense, the writhe is a measure for the internal linking of vortex filaments for a *locally* untwisted bundle, providing valuable information about the internal topology even when the fine structure can not be directly resolved. Though total helicity is agnostic to how it is encoded in the geometry of the vortex lines, it is useful to distinguish these three geometric contributions: centerline linking $\mathcal{L}$, centerline coiling (or writhing) $\mathcal{W}r$ and local twist Tw. The latter cannot be resolved without looking in the vortex core, so we define the centerline helicity, $\mathcal{H}_c/\Gamma^2 = \sum \mathcal{L}_{ij} + \sum \mathcal{W}r_i$, which we measure directly from the vortex centerline geometry.

Recently, elementary vortex knots and links have been found to be intrinsically unstable in experimental viscous fluids [19] and simulations of Bose-Einstein condensates (BECs) [24]. In both cases, thin-core vortices are seen to spontaneously deform towards a series of local reconnections that untie knots and disconnect linked rings. Thin-core vortices of this type are ideal model systems for studying the conservation of helicity; they concentrate the region of interest to a small subset of the broader three-dimensional flow, while efficiently encoding the fundamental physics of the problem in their three-dimensional shape. Indeed, from their shape, physical quantities such as energy, momentum and helicity can be determined [25], and the geometric nature of the description allows natural generalizations to other knotted physical systems. Here, we generate knots, links, and unknots (distorted rings) in vortices in water, simulations of Gross-Pitaevski equation (GPE, a simple model of a BEC [23]), and Biot-Savart simulations, and recon-

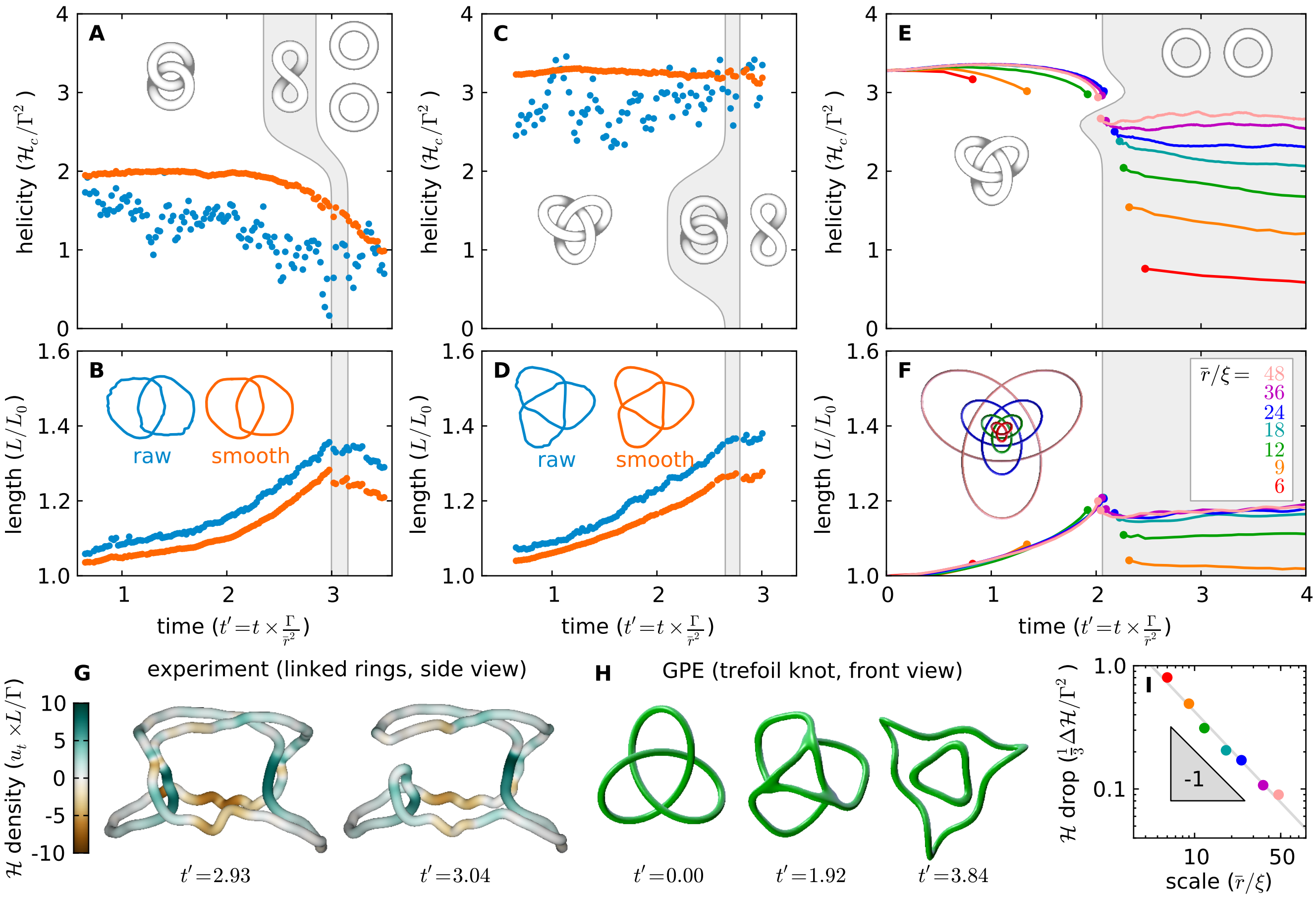

FIG. 2: (**A, B**) The computed center-line helicity ($\mathcal{H}_c$) and length for of a pair of linked rings in experiment through the first two reconnection events, showing the efficient conversion of link helicity to writhing (coiling). The teal data indicates the raw experimental traces, while the orange data has been smoothed with a windowed sinc function whose spatial cutoff is $\lambda = 50$ mm (the total vortex length is $\sim$1 m). The gray inset diagrams indicate the topologies at different stages of the vortex evolution. (**C, D**) The center-line helicity and length for an experimental trefoil vortex knot, through the first two reconnections (out of three total). (**E, F**) The center-line helicity and relative length for GPE-simulated trefoil knots for a range of structure to core-size ratios, $\bar{r}/\xi$. Unlike the experimental results, a clear jump in helicity is observed during the reconnection. The inset shows four color-coded scales, where the tube width corresponds to the healing length, ξ. (**G**) Two traces of a pair of initially linked vortices in experiment, just before and after a reconnection event. The traces are colored according to the computed local helicity density, $h = L/\Gamma u_t$. The change in topology has a small effect on the overall helicity due to the anti-parallel vortex configuration. (**H**) Renderings of density iso-surfaces ($\rho = 0.5\rho_0$) for a trefoil vortex knot ($\bar{r} = 12\xi$), simulated with the GPE. The initially knotted configuration changes to a pair of unlinked rings whose writhe conserves most of the original helicity. (**I**) The helicity jump per reconnection event as a function of size ratio for GPE simulated trefoil knots.

struct the shape of their vortex cores up to and through topology-changing reconnections.

Technical details for all systems are described in the supplementary methods section, and follow established methods [19, 24, 26, 27]. For all systems, the time-dependent vortex shape is reduced to a series of 3D polygonal paths (typically with $\sim 10^3$ points per time step), which are used to calculate all subsequent quantities of interest. For experimental data, the vortices are reconstructed by identifying and tracing line-like features in the volumetric data [28–30]. For the GPE simulations, the vortex paths are obtained by tracing minimal ridges in the density field. While viscous vortices and GPE-simulated BECs allow for vortex reconnections, thin-core Biot-Savart vortices do not, and so we limit the use of these simulations to study the evolution of vortices that are not changing topology. To allow comparisons between different systems, the time of each is rescaled with the r.m.s vortex size, $\bar{r}$, and circulation, Γ: $t' = t \times \Gamma/\bar{r}^2$. For experimental vortices, the circulation is estimated as that of a thin plate in uniform flow [31].

Typically, a reconnection event is expected to violate the conservation of helicity because it changes vortex topology by creating or removing a crossing (e.g. Fig. 1**A**), which should result in a sudden, discontinuous jump of the helicity, $|\Delta\mathcal{H}_c| \sim 1\ \Gamma^2$. Recently, more de-

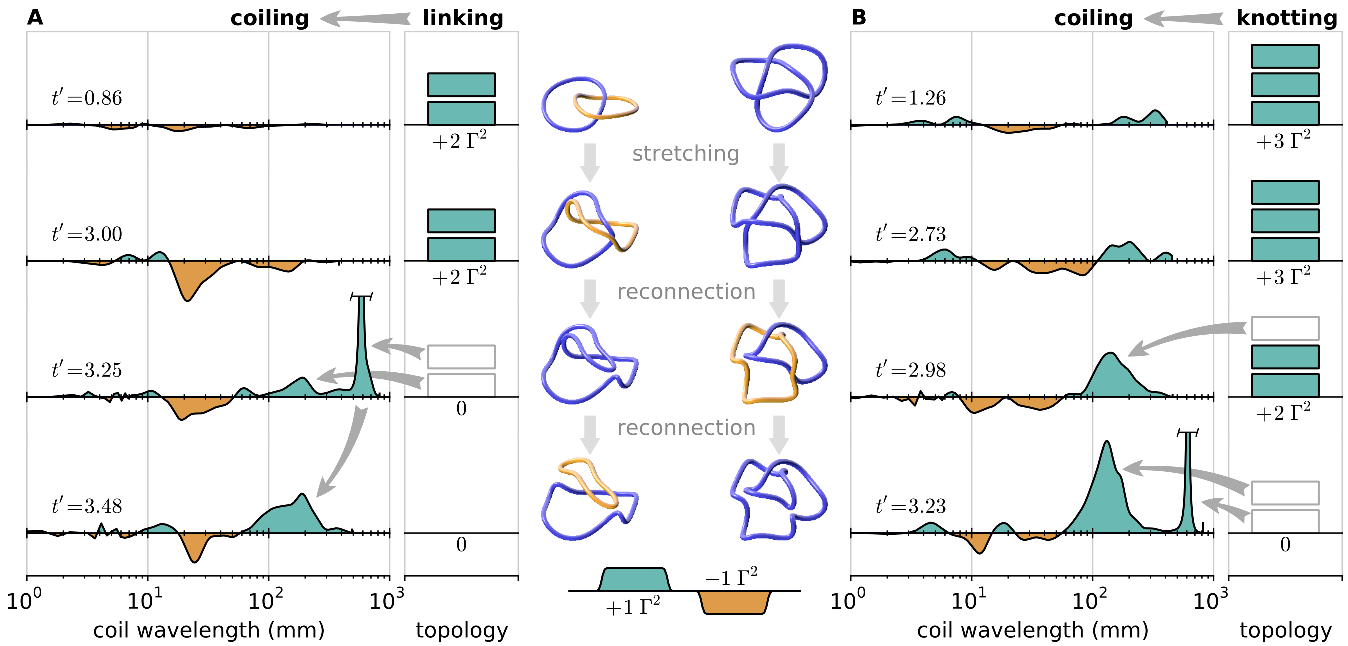

FIG. 3: (**A, B**) 'Helistograms' for **A**, a pair of linked rings and **B**, a trefoil knot in a viscous fluid experiment (the data set is the same as shown in Fig. 2**C-F**; the total vortex length is $\sim$ 1m for both). The left portion of each series of plots shows the helicity contribution due to coiling on different spatial scales, obtained by computing $\partial_n \mathcal{H}_c(\lambda = 10^n)$, where λ is the cutoff wavelength for a windowed sinc smoothing. The right portion of each plot shows the irreducible contribution to the helicity originating from the global vortex topology. Both the coiling and topological contributions are scaled so that the total helicity is proportional to the filled area of the plots. The center column shows images of the numerically traced vortices smoothed to $\lambda = 100$ mm.

tailed analytical results have also indicated that helicity may be dissipated in a reconnection event [17]. Remarkably, results from both our experiments and numerical models reveal jumps in centerline helicity that are significantly smaller (Fig. 2**ACE**). The centerline helicity of viscous fluid vortices appears to be nearly unaffected by reconnections, while GPE simulations show a jump in the range of $|\Delta \mathcal{H}_c| \sim (0.1-0.8)\ \Gamma^2$ which depends on the overall scale of the vortex (Fig. 2**I**). This smaller than expected jump indicates that the vortices are spontaneously arranging themselves into a distinctly non-planar geometry which reduces or eliminates the change in helicity that occurs when a reconnection takes place. (The precise mechanism for this will be discussed later.) Due to the fact that the global topology is changing through every reconnection event, this means that in each case the helicity is changing form: converting from global topology to internal structure, which we measure as writhing.

In the case of linked rings, the linking is converted to the writhe of successively one and then two vortex loops, while in the case of a trefoil knot, the helicity flows from writhe to linking and back to writhe. Superimposed with this changes are small-scale Kelvin-waves excited by the vortex generation process, which can be seen to propagate along the vortex knot. To understand the helicity dynamics it is therefore important to account for the separate contribution to the total writhe from each of these length scales. In order to do this we smooth the measured vortex paths using a windowed sinc kernel of varying width, λ, to introduce a hard spatial-cutoff (see supplementary methods), and recalculate the helicity as a function of this smoothing, $\mathcal{H}_c(\lambda)$. The derivative of this function, $\partial\mathcal{H}_c|_\lambda$, then quantifies the helicity content stored at spatial scale λ (see supplemental movies S1-2). The resulting 'helistograms' are shown in Figure 3. Ultimately, there is a component of the helicity that is not removed by even long-scale smoothing; for the relatively simple topologies studied here the resulting writhe is nearly integer. This integer component arises because the path becomes nearly planar and corresponds to the crossing number in this effective planar projection. We refer to the non-integer fraction removed by smoothing as 'coiling' and to the remainder as an effective integer knotting number, akin to linking (Fig. 3). Thus the transfer of helicity from global linking and knotting to coiling on different scales can be quantified through the reconnections.

Figure 3**A** shows the helistogram for experimental linked rings before, during, and after the reconnection process (see also supplemental movie S3). The 'coiling' component of the writhe, which is initially absent, develops a negative peak on a scale of 20-30 mm (the initial total vortex length is ~850 mm) as the vortex stretches and deforms approaching the first reconnection. Immediately following the reconnection, the topological component of the helicity drops by $2\Gamma^2$ as expected; at this moment the vortex centerline is topologically trivial. To compensate, two positive peaks appear in the helistogram: the first at 200 mm corresponds to a single coiling turn found near the reconnection (also seen in Fig. 2**G**), and the second at 600 mm that quantifies the large-scale folding of the resulting unknot (see also supplemental Fig. S2). The second reconnection event transfers this large scale folding to a second feature on the 200 mm scale.

For the case of the trefoil knot (Fig. 3**B**, supplementary movie S4), we observe similar dynamics. A cancellation between positive and negative coils at different scales maintains near constant total helicity as the vortex initially deforms towards reconnections. After the first reconnection event, the topological component drops by 1 and is balanced by a coiling turn at ∼150 mm. At this point, the vortex tube topology is that of linked rings, and the subsequent topological evolution is qualitatively similar to that of the initially linked rings.

How can the efficient conservation of centerline helicity through a reconnection be understood in view of the fact that the global vortex topology is changing? For a nearly planar vortex shape, a reconnection event would be expected to change the helicity by $\Delta\mathcal{H}_c/\Gamma^2 \sim 1$ because it will create or destroy a crossing (e.g. Fig. 1**A**). However, the notion of a 'crossing' only exists for paths projected into a plane; conversely, the observed vortex shapes are extremely non-planar, particularly so in the region near a reconnection. For non-planar paths, the reconnections can happen between two arbitrarily curved anti-parallel segments (Fig. 4**B**), which conserves helicity because it does not create or destroy a crossing in *any* projected plane. In principle, anti-parallel reconnections can also be drawn for planar shapes if they happen away from a crossing (supplemental Fig. S4), but the resulting diagrams are not representative of the shapes we observe forming naturally in vortex evolution. It has previously been observed that an anti-parallel configuration is spontaneously formed for reconnecting regions when they are driven by stretching; energy conservation dictates that sections of vortex loops should anti-align as they approach to reduce the energy per unit length [19]. Thus, remarkably, the reconnection geometry naturally adopted by linked and knotted vortices is precisely the form required to conserve helicity by the introducing writhe (coiling) which compensates for that lost from the global linking and knotting. This mechanism acts at the moment of reconnection as it is a result of the reassociation of the lines that accompanies the reconnection. Related mechanisms have been suggested for reconnections in dissipative plasmas, although in that case linking is rather converted to internal twist [20, 32, 33].

We now turn to a discussion of analogous processes in GPE simulations of linked and knotted vortex loops. Quantum vortices, like those in the GPE or real superfluids, provide an interesting comparison to viscous fluid vortices because the vortex lines are instead defined by quantized phase discontinuities in the superfluid wavefunction [34, 35]. GPE vortices have no fluid in their core and can store no internal structure, thus their topology is entirely quantified by the centerline helicity $\mathcal{H}_c$ (local twist is not possible). Extraction of the vortex centerlines (obtained by ridge-tracing the reduced density core) reveals similar dynamics, including the stretching and anti-alignment of vortices that heralds the reconnection events (Fig. 2**EF**, Fig. S3, supplementary movie S5) . The helicity drop varies as a function of scale; as the vortex r.m.s. radius ($\bar{r}$) is increased relative to the size of the density-depleted 'core' (ξ), the helicity lost to the reconnection is reduced and is consistent with a $\Delta\mathcal{H}_c \propto (\bar{r}/\xi)^{-1}$ dependance (Fig. 2**I**). This variable drop can be explained by the fact that the relatively thicker colliding cores will start the reconnection process sooner, before they have had time to adopt the ideal configuration. It is unclear if the same effect is present in the experiments, due to the difficulties associated with accurately tracking significantly smaller vortices; studies the detailed dynamics of reconnections in super-fluids and classical fluids suggest that there may be differences [36–38].

Interestingly, the helicity of our GPE knot begins to drop *prior* to the reconnection event, and this drop seems to be only weakly affected by scaling, apparently contradicting the notion that helicity is perfectly conserved in the absence of topology changes. This effect can also be seen in experiments and simulations of distorted vortices when they are not changing topology (for example, the experimental linked rings, Fig. 2**A**). A more dramatic example of this effect can be seen in Biot-Savart simulations of a helically wound ring 'leap-frogging' an undistorted ring. As it passes through the circular ring, the helically wound vortex is compressed and the centerline helicity increases dramatically, even though the global topology does not change (Fig. 4**EF** and supplementary movie S6).

A simple model of this geometric change in centerline helicity can be obtained by considering the writhe of an isolated spring-like helix: $Wr_{\rm helix} \approx \Gamma^2 N \frac{2\pi^2 a^2}{L^2}$, where N is the number of helical turns, a is the radius of the cylinder around which it is wound, L the cylinder length. If this this helix is stretched along the axis by a uniform incompressible flow, this helicity would scale like $\mathcal{H}_{\rm helix} \propto L^{-3}$. This simplistic model qualitatively captures the centerline helicity of the leap-frogging helix of Fig. 4**E**.

On the other hand, if we imagine wrapping a ribbon around a cylinder N times (Fig. 4**D**), we expect the total number of twists in the ribbon to remain constant even if the cylinder changes shape. If we regard the ribbon normal as a method for keeping track of the internal structure of a vortex core, we would conclude the total helicity is constant: $\mathcal{H}_{tot} = N\Gamma^2 = Wr_{\rm helix} + \mathcal{H}_\tau$, where $\mathcal{H}_\tau$ is the twist contribution to the helicity. As

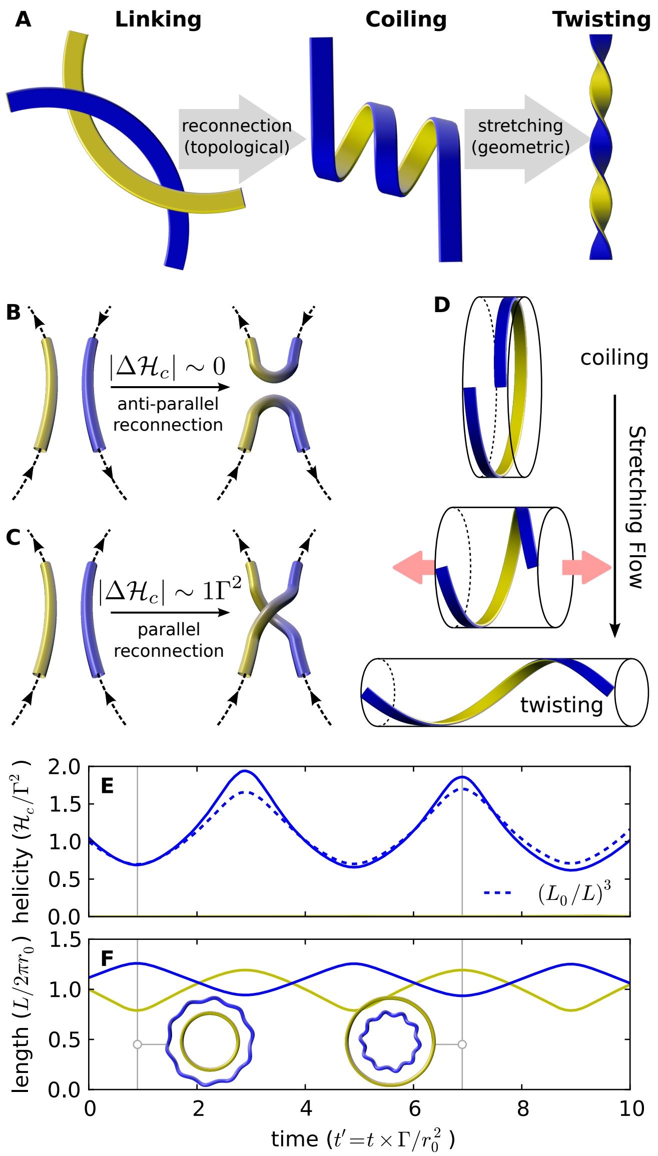

FIG. 4: (**A**) Illustrations of mechanisms for storing helicity on different spatial scales; in each case the helicity of the depicted region is the same, $\mathcal{H}_c = 2\Gamma^2$. While linking is global in nature, both coiling and twisting are local – they produce linking between different sub-sections of the vortex tube, or in this case different edges of the illustrated ribbon. (**B, C**) Diagrams of reconnection events in locally anti-parallel or parallel orientations. The anti-parallel reconnection does not change helicity because it does not introduce a new 'crossing' of the projected tubes, unlike the parallel reconnection. This anti-parallel configuration tends to form spontaneously for topologically non-trivial vortices, even in the absence of viscosity, in which case helicity is efficiently converted from global linking to local coiling. (**D**) Coiling can be converted to twisting by stretching helical regions of the vortex; this mechanism conserves total helicity because it does not change the topology, and results in an apparent change of helicity when core-twist can not be resolved. (**E, F**) The helicity (**E**) and length (**F**) as a function of time for a simulated geometrical evolution of a circular vortex ring (yellow) 'leap-frogging' a vortex ring with a helix superimposed (blue).

shown above, the writhe contribution varies as the vortex is stretched, and so we see that stretching provides a purely geometric mechanism for converting coiling to twist helicity. In the case of the GPE simulation, the vortex core does not support structure and so there can be no such conversion; the helicity will then vary as the vortex is stretched. For experimental vortices, this twist should be present but we are not able to directly resolve it; doing so is a challenging goal for future investigations.

Ultimately, when should one expect helicity to be dissipated for viscous vortices? For Navier-Stokes flow, the rate of change of helicity is given by: [1]

$$\partial_t \mathcal{H} = -2\nu \int \boldsymbol{\omega} \cdot (\boldsymbol{\nabla} \times \boldsymbol{\omega})\, dV, \tag{4}$$

where ν is the kinematic viscosity of the fluid. For a straight, uniformly twisted section of vortex tube, the dissipation rate is then given by $\partial_t \mathcal{H} = -\mathcal{H}_\tau \frac{\nu}{A_{eff}}$, where A_{eff} is an effective core area (see supplemental information for details). In other words, the helicity is dissipated when the core is *locally* twisted. As a result, helicity is viscous vortices only stably stored as knots, links, or coils, but not as local twist. This is notable because twist helicity is also not present for GPE vortices (or quantum vortices more generally), suggesting an interesting correspondence in their topological dynamics.

Our results show that helicity can be conserved in real fluids even when their vortex topology is not. Vortex reconnections do not simply dissipate helicity, but rather mediate a flow from knotting and linking on large scales to coiling on smaller scales. Related geometric mechanisms may convert this coiling into twist on even smaller scales, where it may be dissipated. Interestingly, both topological (Fig. 4**B**) and non-topological (Fig. 4**D**) mechanisms for helicity transport are driven by stretching, which is observed to happen spontaneously for initial linked or knotted vortices. As these mechanisms we identify have a natural geometric interpretation, they readily extend to any topological flow. Taken as a whole, this suggests that helicity may yet be a fundamental conserved quantity, guiding the behavior of dissipative complex flows from braided plasmas to turbulent fluids.

The authors acknowledge the MRSEC Shared Facilities at the University of Chicago for the use of their instruments. This work was supported by the National Science Foundation (NSF) Materials Research and Engineering Centers (MRSEC) Program at the University of Chicago (DMR-0820054). W.T.M.I. further acknowledges support from the A.P. Sloan Foundation through a Sloan fellowship, and the Packard Foundation through a Packard fellowship.

---

[*] These two authors contributed equally.

[†] Electronic address: dkleckner@uchicago.edu

[‡] Electronic address: wtmirvine@uchicago.edu

[1] Moffatt, H. K. Degree of Knottedness of Tangled Vortex Lines. *Journal of Fluid Mechanics* **35**, 117–129 (1969).

[2] Thomson, W. On vortex atoms. *Philosophical magazine* **XXXIV**, 94–105 (1867).

[3] Moffatt, H. K. Helicity and singular structures in fluid dynamics. *Proceedings of the National Academy of Sciences of the United States of America* **111**, 3663–70 (2014).

[4] Ricca, R. L. & Berger, M. A. Topological ideas and fluid mechanics. *Physics Today* **49**, 28–34 (1996).

[5] Tkalec, U. *et al.* Reconfigurable Knots and Links in Chiral Nematic Colloids. *Science* **333**, 62–65 (2011).

[6] Martinez, A. *et al.* Mutually tangled colloidal knots and induced defect loops in nematic fields. *Nature materials* **13**, 258–63 (2014).

[7] Dennis, M. R., King, R. P., Jack, B., O'holleran, K. & Padgett, M. Isolated optical vortex knots. *Nature Physics* **6**, 118–121 (2010).

[8] Kedia, H., Bialynicki-Birula, I., Peralta-Salas, D. & Irvine, W. T. M. Tying Knots in Light Fields. *Physical Review Letters* **111**, 150404 (2013).

[9] Han, D., Pal, S., Liu, Y. & Yan, H. Folding and cutting DNA into reconfigurable topological nanostructures. *Nature nanotechnology* **5**, 712–717 (2010).

[10] Chichak, K. S. *et al.* Molecular borromean rings. *Science* **304**, 1308–12 (2004).

[11] Sumners, D. Lifting the curtain: Using topology to probe the hidden action of enzymes. *Notices of the American Mathematical Society* 528–537 (1995).

[12] Vachaspati, T. & Field, G. Electroweak string configurations with baryon number. *Physical review letters* **73**, 373–376 (1994).

[13] Bekenstein, J. D. Conservation law for linked cosmic string loops. *Physics Letters B* **282**, 44–49 (1992).

[14] Faddeev, L. & Niemi, A. Stable knot-like structures in classical field theory. *Nature* **387**, 58–61 (1997).

[15] Bewley, G. P., Paoletti, M. S., Sreenivasan, K. R. & Lathrop, D. P. Characterization of reconnecting vortices in superfluid helium. *Proceedings of the National Academy of Sciences of the United States of America* **105**, 13707–10 (2008).

[16] Cirtain, J. W. *et al.* Energy release in the solar corona from spatially resolved magnetic braids. *Nature* **493**, 501–3 (2013).

[17] Kimura, Y. & Moffatt, H. K. Reconnection of skewed vortices. *Journal of Fluid Mechanics* (2014).

[18] Kida, S. & Takaoka, M. Reconnection of vortex tubes. *Fluid Dynamics Research* **3**, 257–261 (1988).

[19] Kleckner, D. & Irvine, W. T. M. Creation and dynamics of knotted vortices. *Nature Physics* **9**, 253–258 (2013).

[20] Pfister, H. & Gekelman, W. Demonstration of helicity conservation during magnetic reconnection using Christmas ribbons. *Am. J. Phys* **59**, 497–502 (1991).

[21] Moffatt, H. & Ricca, R. Helicity and the Calugareanu invariant. *Proceedings of the Royal Society A: Mathematical, Physical and Engineering Sciences* **439**, 411 (1992).

[22] Berger, M. A. Topological Quantities: Calculating Winding, Writhing, Linking, and Higher order Invariants. In Ricca, R. L. (ed.) *Lectures on Topological Fluid Mechanics*, vol. 1973 of *Lecture Notes in Mathematics*, 75–97 (Springer Berlin Heidelberg, Berlin, Heidelberg, 2009).

[23] Pitaevskii, L. P. & Stringari, S. *Bose-Einstein Condensation* (Clarendon Press, Oxford, 2003).

[24] Proment, D., Onorato, M. & Barenghi, C. Vortex knots in a Bose-Einstein condensate. *Physical Review E* **85**, 1–8 (2012).

[25] Donnelly, R. J. Vortex rings in classical and quantum systems. *Fluid Dynamics Research* **41**, 051401 1–31 (2009).

[26] Berloff, N. G. Padé approximations of solitary wave solutions of the GrossPitaevskii equation. *Journal of Physics A: Mathematical and General* **37**, 1617–1632 (2004).

[27] Salman, H. Breathers on Quantized Superfluid Vortices. *Physical Review Letters* **111**, 165301 (2013).

[28] Eberly, D. *Ridges in Image and Data Analysis* (Springer, 1996).

[29] Kindlmann, G. L., Estépar, R. S. J., Smith, S. M. & Westin, C.-F. Sampling and Visualizing Creases with Scale-Space Particles. *IEEE Trans. Visualization and Computer Graphics* **15**, 1415–1424 (2009).

[30] Sethian, J. A. A fast marching level set method for monotonically advancing fronts. *Proceedings of the National Academy of Sciences of the United States of America* **93**, 1591–5 (1996).

[31] Acheson, D. J. *Elementary Fluid Dynamics* (Clarendon Press, Oxford, 1990).

[32] Lau, Y. & Finn, J. Magnetic reconnection and the topology of interacting twisted flux tubes. *Physics of Plasmas* **3**, 3983 (1996).

[33] Berger, M. A. & Field, G. B. The topological properties of magnetic helicity. *Journal of Fluid Mechanics* **147**, 133 (2006).

[34] Onsager, L. Statistical Hydrodynamics. *Nuovo Cimento* **Vl**, 249 (1949).

[35] Feynman, R. Application of Quantum Mechanics to Liquid helium. *Progress in low temperature physics* **1**, 17–53 (1955).

[36] Kerr, R. M. Vortex Stretching as a Mechanism for Quantum Kinetic Energy Decay. *Physical Review Letters* **106**, 224501 (2011).

[37] Donzis, D. a. *et al.* Vorticity moments in four numerical simulations of the 3D Navier-Stokes equations. *Journal of Fluid Mechanics* **732**, 316–331 (2013).

[38] Paoletti, M., Fisher, M., Sreenivasan, K. & Lathrop, D. Velocity Statistics Distinguish Quantum Turbulence from Classical Turbulence. *Physical Review Letters* **101**, 154501 (2008).